doi:10.1016/j.jmb.2003.09.064 J. Mol. Biol. (2003) 334, 445–458

JMB

Available online at www.sciencedirect.com

SCIENCE DIRECT®

ELSEVIER

The Solution Structure of Human Mitochondria Fission Protein Fis1 Reveals a Novel TPR-like Helix Bundle

Motoshi Suzuki[1], Seon-Yong Jeong[1], Mariusz Karbowski[1] Richard J. Youle[1] and Nico Tjandra[2]*

[1]*Biochemistry Section, Surgical Neurology Branch, National Institute of Neurological Disorders and Stroke, National Institutes of Health, Bethesda MD 20892, USA*

[2]*Laboratory of Biophysical Chemistry, National Heart Lung, and Blood Institute Building 50, Room 3503, 50 Center Drive, Bethesda, MD 20892-8013, USA*

**Corresponding author*

Fis1 in yeast localizes to the outer mitochondrial membrane and facilitates mitochondrial fission by forming protein complexes with Dnm1 and Mdv1. Fis1 orthologs exist in higher eukaryotes, suggesting that they are functionally conserved. In the present study, we cloned the human Fis1 ortholog that was predicted in a database, and determined the protein structure using NMR spectroscopy. Following a flexible N-terminal tail, six α-helices connected with short loops construct a single core domain. The C-terminal tail containing a transmembrane segment appears to be disordered. In the core domain, each of two sequentially adjacent helices forms a hairpin-like conformation, resulting in a six helix assembly forming a slightly twisted slab similar to that of a tandem array of tetratricopeptide repeat (TPR) motif folds. Within this TPR-like core domain, no significant sequence similarity to the typical TPR motif is found. The structural analogy to the TPR-containing proteins suggests that Fis1 binds to other proteins at its concave hydrophobic surface. A simple composition of Fis1 comprised of a binding domain and a transmembrane segment indicates that the protein may function as a molecular adaptor on the mitochondrial outer membrane. In HeLa cells, however, increased levels in mitochondria-associated Fis1 did not result in mitochondrial translocation of Drp1, a potential binding partner of Fis1 implicated in the regulation of mitochondrial fission, suggesting that the interaction between Drp1 and Fis1 is regulated.

Keywords: mitochondria; NMR; dynamin; Tom20; Tom70

Introduction

Mitochondria play a major role in metabolism, ATP production, and apoptosis. Their abundance as well as shape appear to be important for cellular vitality. Maintenance of mitochondrial copy number and morphology depend on the balance between fusion and fission events, and are regulated by several proteins. Mitochondrial fusion in mammals is regulated by transmembrane GTPases, Mfn1 and Mfn2,[1] first identified as Fzo1 in fly[2] and yeast.[3,4] Mitochondrial fusion is counterbalanced by fission mediated by Drp1, first identified as Dnm1 in yeast.[5–7] Dnm1/Drp1 is a dynamin-related, cytosolic GTPase that translocates to mitochondrial outer membranes during mitochondrial fission[5,8] and during apoptosis.[9]

The Dnm1-dependent fission event in yeast is accomplished with two other proteins, Fis1 and Mdv1.[10–12] These three proteins are in a high-order complex that constructs a punctate structure at the dividing site of the mitochondrial outer membrane surface. A proposed molecular mechanism for mitochondrial fission describes two separate steps mediated by Fis1.[11] Initially Fis1 regulates the assembly of Dnm1 into punctate structures. Subsequently interaction between Fis1 and Mdv1 regulates the Dnm1-involved constriction and division of mitochondrial membrane. Interestingly, homologs of Mdv1 have not been identified in higher eukaryotes, and it is unknown if another protein takes its place or if Mdv1 function is not

Abbreviations used: TPR, tetratrico-peptide repeat; NOE, nuclear Overhauser effect; RMSD, root mean squared deviation.

E-mail address of the corresponding author: nico@helix.nih.gov

necessary for mitochondria fission in higher eukaryotes. However, the presence of Fis1 homologs in higher eukaryotes is predicted, suggesting that its role in mitochondrial fission is conserved during evolution.

Yeast Fis1 is an integral membrane protein of 17 kDa in size, with the N terminus exposed to the cytoplasm and a single transmembrane segment at its C terminus.[10] These characteristics appear to be conserved in human Fis1, but no additional structural or functional motif is found in the amino acid sequence of yeast or human Fis1 to suggest the protein function at the molecular level.

Here, we present the three-dimensional protein structure of human Fis1. Although no known structural motif was found in its amino acid sequence, we unexpectedly found that the folding of Fis1 is similar to the way multiple tetratrico-peptide repeat (TPR) motifs fold. The TPR[13,14] contains degenerate 34 amino acid sequences with eight loosely conserved consensus residues. The TPR motif is found in a wide variety of proteins with divergent cellular functions. TPRs are usually present in a tandem array of multiple motifs. TPR-containing domains mediate protein–protein interactions as part of large assemblies, but the common features in the interaction partners have not been defined. On the basis of the structural information of Fis1 that consists of a TPR-like domain and a C-terminal transmembrane region, we propose that human Fis1 functions as a molecular adaptor in the process of mitochondrial fission.

Results

Protein sequence, secondary structure, and backbone dynamics

In the previous report,[10] a human ortholog of yeast Fis1 was identified by a database search, with genebank accession number NP057152. Using BLAST, we have identified two orthologs in humans, NP07152 and AAH03540, with only two amino acid differences (Thr45Arg46 and Ser45Lys46, respectively). We have cloned a cDNA from hepatocellular carcinoma Hep G2 cells. Sequence analysis revealed that it is identical with AAH03540. Another clone was obtained from brain tissue, and the sequence was exactly the same as AAH03540. The protein translated from the cloned cDNA is hereinafter called human Fis1. The amino acid sequence of human Fis1 is compared to that of yeast Fis1[10,11] and those of predicted orthologs of other species. The region corresponding to residue Met1 to Val30 of human Fis1 is the least similar to that of lower eukaryotes. The rest of the protein shows higher sequence identity and conservation among Fis1 orthologs, resulting in overall sequence similarity of 40% between yeast and human Fis1. Fis1 sequences from mammals show a significantly higher similarity, and human Fis1 shares 98% sequence homology against the mouse counterpart, including Ser45Lys46. Fis1 orthologs contain a hydrophobic stretch at their C termini, considered to be a transmembrane region. Sequence similarity to proteins outside of the Fis1 ortholog family cannot be found in the current databases.

The secondary structure of human Fis1, derived from a combination of NMR data typically used for identification of secondary structure, is indicated in Figure 1. The NMR data obtained for the recombinant protein along with the location of secondary elements are shown in Figure 2. Six α-helices, of roughly equivalent length, are defined based on nuclear Overhauser effects (NOEs) between $H^N(i)$ and $H^N(i+1)$, between $H^\alpha(i)$ and $H^N(i+3)$, and between $H^\alpha(i)$ and $H^\beta(i+3)$, on $^{13}C^\alpha$ secondary chemical shifts, and on ϕ and ψ dihedral angles (not shown). These angles are based on the $^{13}C^\alpha$, $^{13}C^\beta$, $^{13}C'$, $^1H^\alpha$, and $^{15}N^H$ chemical shifts using TALOS program.[15] The carboxy ends of α1, α3, α5, and α6 helices were not well defined

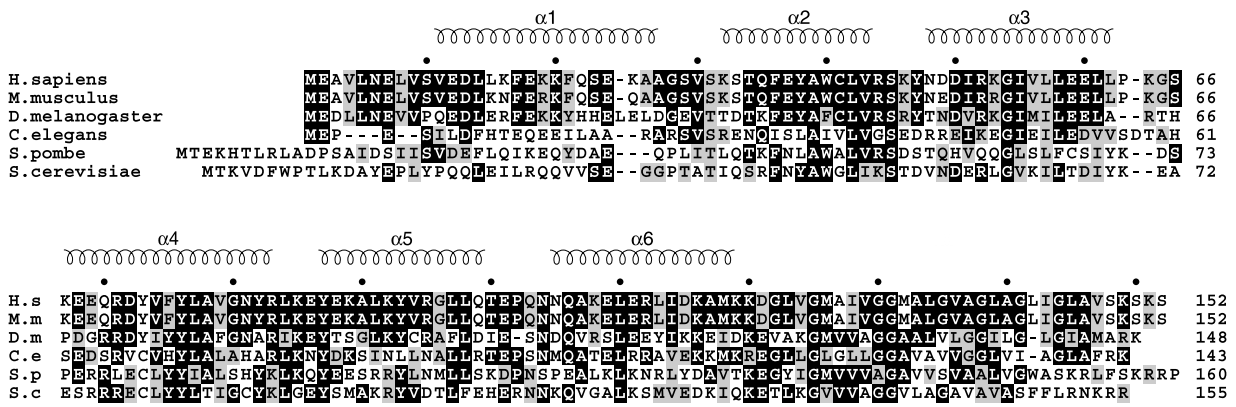

Figure 1. The amino acid sequence comparison of Fis1 orthologs. The sequences are obtained from NCBI database with accession numbers NP 012199 for *Saccharomyces cerevisiae*, NP 595719 for *Schizosaccharomyces pombe*, NP 495381 for *Caenorhabditis elegans*, AAM68368 for *Drosophila melanogaster*, NP 079838 for *Mus musculus*, and AAH03540 for *Homo sapiens*. The sequences are aligned using ClustalW,[49] and stylized using BoxShade Utility. The secondary structure of human Fis1 is indicated above its sequence.

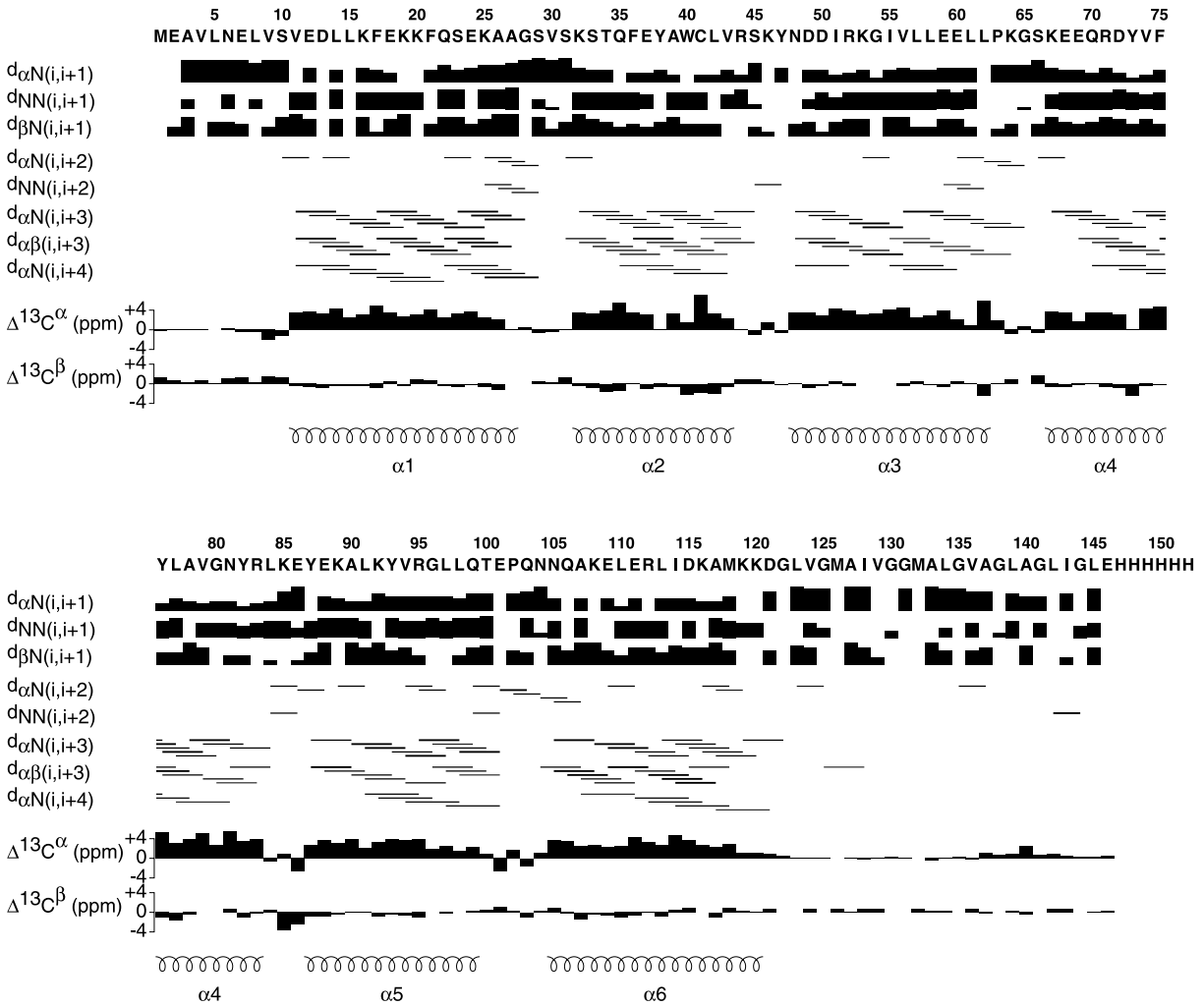

Figure 2. Data obtained using NMR spectroscopy to establish the secondary structure of human Fis1. Sequential and medium-range NOE connectivities characteristic of α-helices as well as $^{13}C^{\alpha}$ and $^{13}C^{\beta}$ secondary shifts are presented along with the amino acid sequence. The location of the different helices in the sequence is indicated. The C-terminal seven residues of the sequence are non-native, but the length of the sequence for the recombinant protein is the same as that for the native protein. The height of bars for NOE connectivities presentation indicates the NOE intensity. The absence of typical NOEs within the α-helical regions mostly means that data were not included due to difficulty of picking overlapped peaks. The height of the bars for secondary shifts presentation are the difference from the random coil values.

due to disagreement of different data sets. Here, we define helix α1 for residues Val11-Ala27, α2 for Lys32-Val43, α3 for Asn48-Leu62, α4 for Lys67-Tyr83, α5 for Tyr87-Thr100, and α6 for Asn105-Lys120. The hydrophobic stretch at the carboxy terminus of the recombinant protein does not appear to adopt a known secondary structure, probably as a result of the frequent appearance of glycine residues.

Backbone relaxation data are shown in Figure 3. The data provide a good indication that Fis1 exists as a monomer in solution as the average ^{15}N T_2 value for residues in regular secondary structures is characteristic for a protein of this size. The backbone ^{15}N T_2 values were used to identify flexible regions in the protein. A marked increase in ^{15}N T_2 indicates that the N-terminal tail is highly mobile. The loops between helices are quite rigid except for the one located between helix α1 and α2 (residues Gly28-Ser31), that appears to be flexible. The backbone dynamic data for the C-terminal region provide unordinary values. The continuous increase in ^{15}N T_2 values along with the increase in residue number had been expected for the flexible C-terminal tail. However, after the gradual increase from residue number 121 to 126, the ^{15}N T_2 values stay within the range of 0.06–0.13 seconds. The C terminus seems neither highly flexible as a typical random coiled tail nor rigid as a stable structural domain.

The three-dimensional structure description

The structure of Fis1 was determined using distance restraints translated from signal intensities of proton homonuclear NOEs, with supplemental vector restraints from residual dipolar couplings. The NMR derived structures of Fis1 are presented

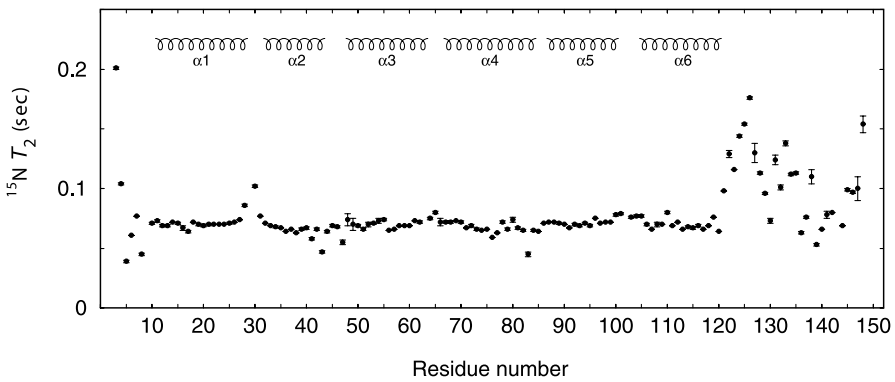

Figure 3. Backbone dynamics of human Fis1. Transverse relaxation rate for the backbone amides of human Fis1 are plotted as a function of residue number. Location of secondary structure elements is indicated.

in Figure 4. As seen in the ensemble of the 20 lowest energy structures, the N-terminal seven residues were not well defined, which is in agreement with backbone dynamic data. There is no long-range NOE within the residues Met1-Asn6. The C^{α} and C^{β} chemical shifts for residues Met1-Ser10 are close to their random coil values (Figure 2). The N terminus therefore does not adopt an ordered conformation in solution. In contrast, the rigid region of the protein (residues Val11-Lys120) was well defined. The atomic RMSD value about the mean of coordinates for six helices was 0.5(±0.1) Å for backbone heavy atoms and 1.0(±0.1) Å for all heavy atoms. No distance and dihedral restraints consistently violated more than 0.4 Å and 5°, respectively.

The six helices construct one core domain. The shape of the core domain is a slightly curved rectangle slab. Sequentially adjacent helix pairs align in anti-parallel fashion, and all six helices reside in a single plane. The thickness of the slab is slightly more than twice of the diameter of an α-helix, and the slab is curved so that one side is concave and the other is convex (Figure 4B).

The C-terminal region is not well defined. Some proton–proton NOEs were observed between this C-terminal region and the concaved surface of the core domain. These include NOEs between Ile143 and Phe75, Tyr76, or Val79. However, the backbone relaxation data suggest that the C-terminal tail is not as stable as the core domain. The data suggest that the C-terminal tail transiently interacts with the core domain. Therefore, such NOEs were excluded from the structure calculation, resulting in a disordered structure for the C-terminal tail.

The helix folding of Fis1 structure

The absence of sequence similarity between Fis1 and other proteins with known functions prohibits reasonable prediction of its biological function. In order to investigate the structure-based function of Fis1, a search for folding similarity was performed using the DALI program[16] against a representative set of structures in the PDB database. The DALI search revealed that the folding of the six helices appearing in the core domain of human Fis1 is often seen in helix-rich proteins. A list of proteins with similar folding was shortened according to the strength of structural similarity (Z score > 6), the total number of corresponding residues (LALI > 100), and the continuity of the corresponding residues. The short list includes 1FCH (C-terminal domain of PEX5[17]), 1A17 (N-terminal domain of PP5[18]) and 1QQE (Sec17,[19] a yeast homolog of mammalian α-SNAP).

The domains in the above proteins contain a tandem repeat of TPR motifs, where one TPR motif forms a helix-turn-helix hairpin. From the structural comparison analyzed by the DALI program (Figure 5), it should be noted that the α2-turn-α3 hairpin of Fis1 corresponds to one of the TPR motifs, and the α4-turn-α5 hairpin corresponds to the next TPR motif. The inter-helical angle between α2 and α3 is 29°, and between α4 and α5 is 25°, comparable to typical inter-helical angle for two helices in a TPR ranging from 23° to 30°.[18–20] Protein stability is achieved by the interaction among hydrophobic residues and by the surface exposure of hydrophilic residues. In the structures of Fis1, PEX5, PP5, and Sec17, some hydrophobic residues that seem to be important for protein core formation are similarly positioned (Figure 5B).

In order to examine whether or not human Fis1 contains a typical TPR motif, the sequences corresponding to the α2-turn-α3 and α4-turn-α5 hairpins of human Fis1 are aligned to the sequences of proteins with a tandem of TPR motifs (Figure 6). From multiple sequence alignments of many known TPR motifs, it is clear that there are no strictly conserved residues within the 34 amino acid-sequences. However, there is a preference for aromatic and hydrophobic amino acid residues at certain positions. On the basis of the appearance of the types of hydrophobic and aromatic residues, it is hard to conclude that the α2-turn-α3 and α4-turn-α5 hairpins of human Fis1 represent two TPR motifs. Nevertheless, based on the structural similarity, we still expect human Fis1 to function as TPR-containing proteins. Although the biological functions of TPR-containing proteins differ, the

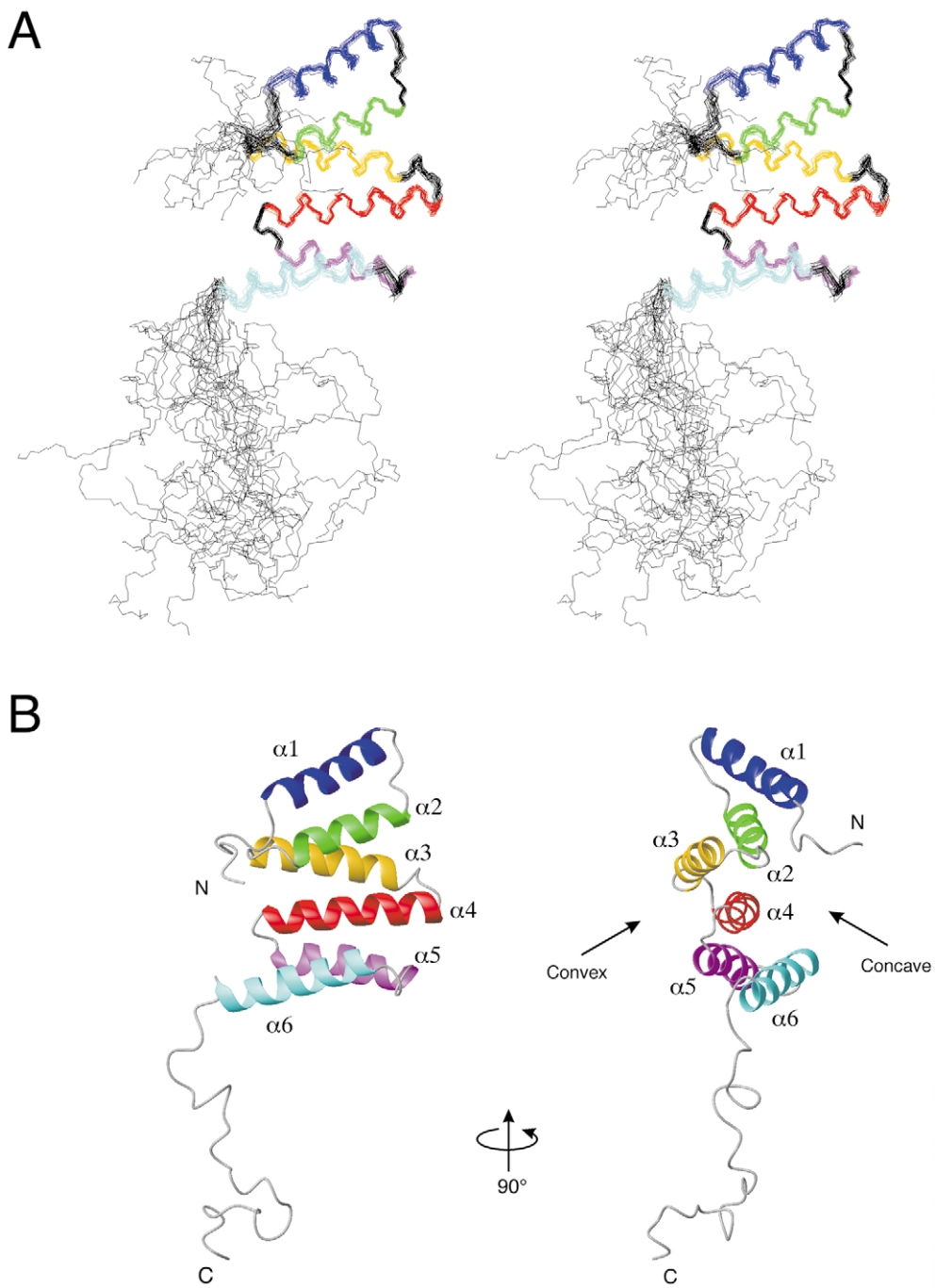

Figure 4. Three-dimensional structure of human Fis1. A, A stereo view of the backbone (N, C^{α}, C′ and O) superposition of 20 NMR derived structures. Helices are distinguished by different colors. Residues Val11-Ala27, Lys32-Val43, Asn48-Leu62, Lys67-Arg83, Tyr87-Thr100, Asn105-Lys120 make up helices α1 (blue), α2 (green), α3 (orange), α4 (red), α5 (magenta), α6 (cyan), respectively. B, Ribbon representations of an averaged minimized NMR structure. The view on the left has the same orientation as A, while the right view has been rotated 90° about the vertical axis. The six helices are color-coded as in A. The letters N and C indicate the N and C termini, respectively. The concave and convex sides of the twisted sheet of helices are indicated in the right panel, while the concave side is viewed in the left panel. Molecular representations were generated using MOLMOL.[46]

TPR domains mediate protein–protein interaction essential to their biological function.

Non-TPR proteins are also listed by the DALI search, although they have lower Z-scores, lower LALI, or discontinuous corresponding residues. These include 1QJA (14-3-3 isoform ζ[21]) and 1OM2 (the cytosolic domain of TOM20[22]). TOM20 is not listed in the NCBI Conserved Domain Database for TPR, but it appears to have a single TPR motif with loosely conserved consensus residues,[22,23] whereas the TPR motif usually occurs as a tandem array of many repeats. Corresponding regions of

A

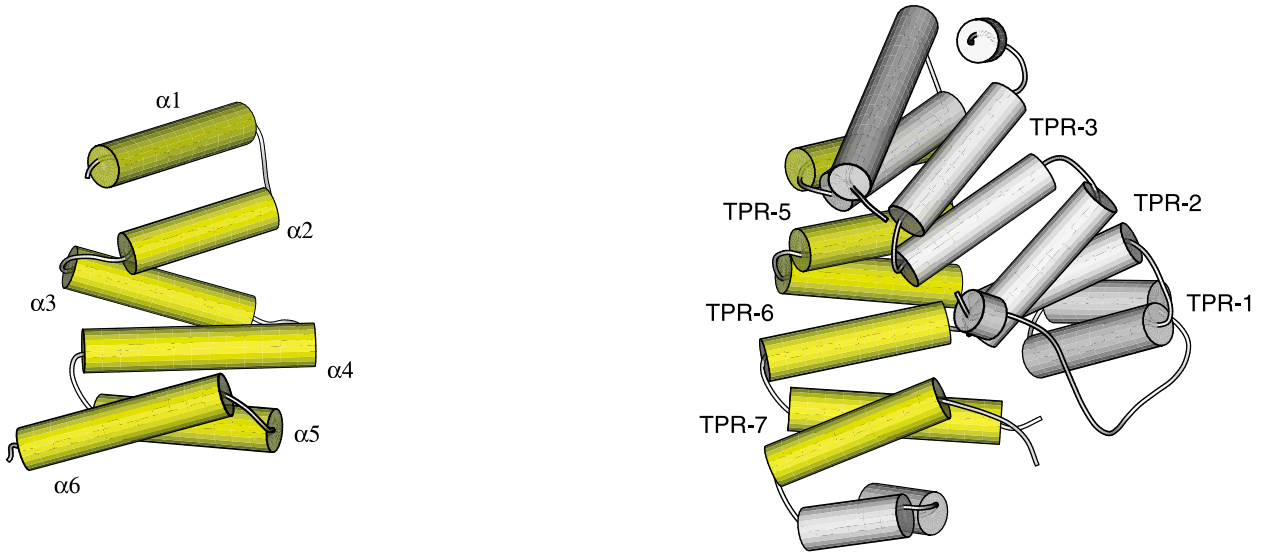

B

```
                α1                  α2                  α3                  α4                  α5                  α6
Fis1    sVEDLLKFEKKFQSEKAAgsvsKSTQFEYAWCLVrskyNDDIRKGIVLLEELLpkgsKEEQRDYVFYLAVGNYRlkeYEKALKYVRGLLQTepqnNQAKELERLIDKAMKKd
1FCH    YDKAVDCFTAALSVrp----ndYLLWNKLGATLANgn---qSEEAVAAYRRALELq--pgyIRSRYNLGISCINLgaHREAVEHFLEALNMQRmsENIWSTLRLALSMLgq-
1A17    kakdYENAIKFYSQAI-ELnpnAIYYGKRSLAYLRt---ecYGYALGDATRAIELdk--kyIKGYYRRAASNMAlgkFRAALRDYETVVKVkphdKDAKMKYQECNKIVKQK
1QQE    -kelNLAGDSFLKYQKKagn-AGNTYVEAYKCFKSg---gnSVNAVDSLENAIQIFqFRRGANFKFELGEILENlhdYAKAIDCYELAGEWYALSNKCFIKCADLKALdgq-
        TPR                 TPR                 TPR                 TPR
```

Figure 5. Structural comparison of Fis1 and proteins with similar helix folding. A, Cylinder representation of the core domain of human Fis1 (left) and of the C-terminal domain of PEX5 (right). The coordinate was obtained from the PDB database with accession number 1FCH. Yellow cylinders indicate the corresponding helices to the core domain of human Fis1. Known TPR motifs are indicated. Figures were produced using MOLSCRIPT.[47] B, Corresponding residues of four structures with similar helix folding using DALI.

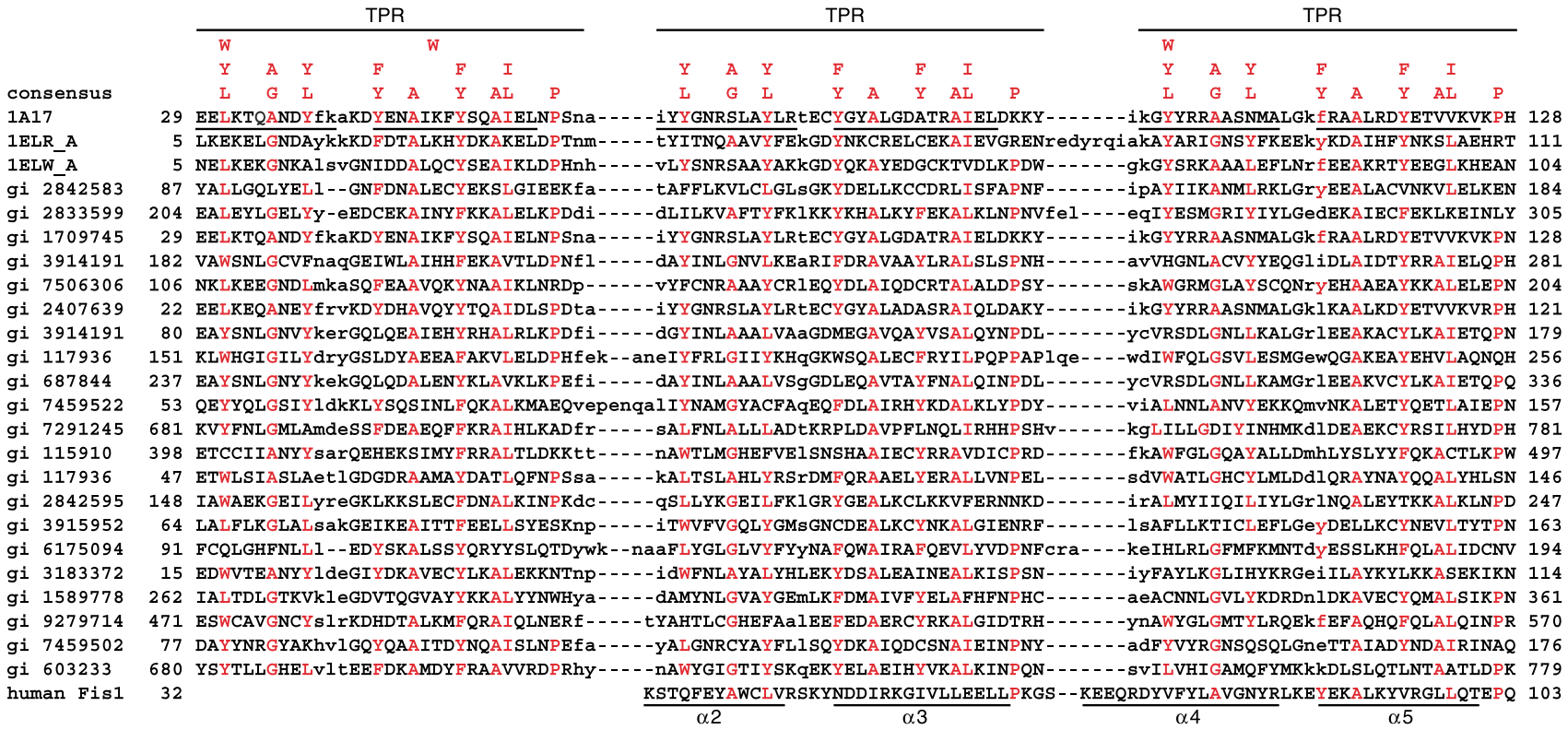

Figure 6. The sequence alignment of Fis1 and other tandem TPR motifs. The arrays of three consecutive TPR motifs were obtained from NCBI Conserved Domain Database (CDD) with accession number cd00189. Letters in red indicate the consensus residues. The consensus sequence in the database is [WFL]-X(2)-[LIM]-[GAS]-X(2)-[YLF]-X(8)-[ASE]-X(3)-[FYL]-X(2)-[ASL]-X(4)-[PKE]. The consensus sequence listed in this Figure is slightly modified for better representation. The sequence from α2-α5 of Fis1 was manually aligned to the above sequences. Underlines indicate the location of secondary structure elements.

14-3-3 ζ and TOM20 are also responsible for protein–protein interactions.

Surface characteristic of Fis1 structure

The folding of helices in Fis1 drives a hypothesis that the protein functions in protein–protein interaction, although the binding partner has not yet been identified for human Fis1. It is useful to consider the surface characteristic of Fis1 in order to investigate a possible binding mechanism. The distributions of hydrophobic residues and of charge are illustrated in Figure 7. There is a concentrated appearance of hydrophobic residues at the groove created on the concave side of the Fis1 structure, as indicated by the arrow in Figure 7A. This suggests the binding with target proteins will be due to hydrophobic interaction at the groove. Only one other highly hydrophobic area is found, that at the C-terminal tail of the protein, which was easily predicted from its sequence. The opposite, convex side of the Fis1 structure shows scattered distribution of hydrophobic residues.

The protein surface with electrostatic potential displays dispersed patches of negative or positive charged areas on the Fis1 structure (Figure 7B).

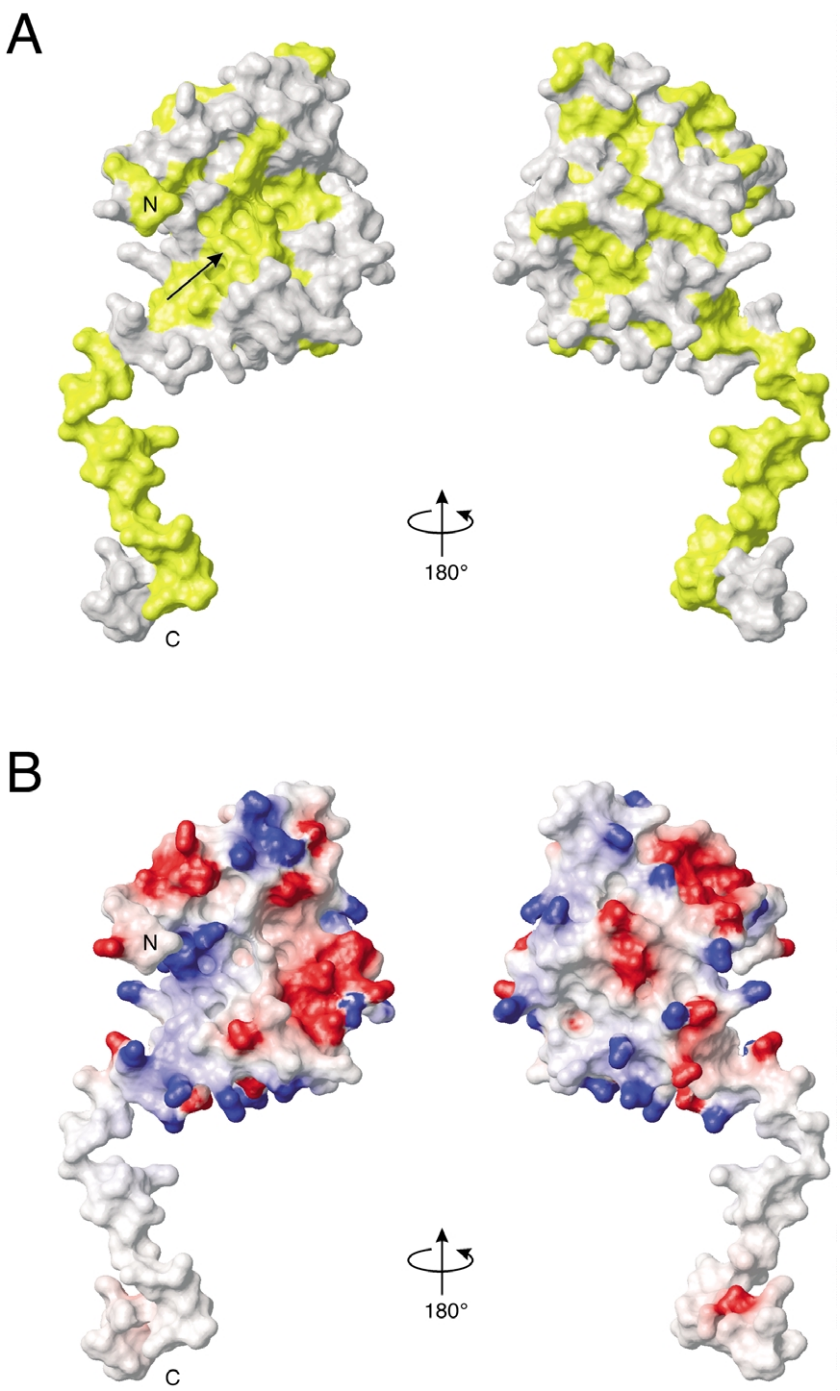

Figure 7. Surface representations of human Fis1. A, The hydrophobic residue distribution around the protein surface. The calculated surface for the averaged minimized structure is colored in yellow when the residue type is alanine, glycine, methionine, tryptophan, tyrosine, phenylalanine, leucine, isoleucine, valine, and proline. The view on the left has the same orientation as Figure 4B left, so that the concave side is viewed, while the right view has been rotated 180° about the vertical axis, so that the convex side is viewed. The arrow indicates the concentrated hydrophobic region described in the text. B, The electrostatic potential surfaces. Positively charged areas are colored blue and negatively charged areas are in red. The views in the two panels are the same orientations as in A. The red color at the C-terminal tip comes from Glu146 that is a cloning artifact. There are two lysine residues at the C-terminal end. Figures were drawn using MOLMOL.[46]

Both negative and positively charged residues exist at the bank of the hydrophobic groove. Charges are evenly distributed around the Fis1 structure so that a simple ionic interaction to target proteins cannot be expected.

C-terminal mitochondria-anchoring domain

The carboxy termini of Fis1 orthologs are characteristic; a stretch of more than 20 residues composed of hydrophobic amino acid residues is sandwiched between positively charged residues (lysine residues and arginine residues). The transmembrane region with this feature is considered to direct proteins to the mitochondrial outer membrane.[24] Yeast Fis1 was found to target and anchor into the mitochondrial outer membrane *via* its C-terminal tail.[10] To determine if the C-terminal tail of human Fis1 is required for mitochondrial localization, we investigated the subcellular location of human Fis1 in living cells (Figure 8) using yellow fluorescence protein (YFP) to report the location of the expressed protein. YFP-Fis1 circumscribed mitochondria completely, indicating that Fis1 localizes at the mitochondrial outer membrane. In contrast, without the C-terminal 30 residues, the expressed protein fails to localize to mitochondria, and is diffuse in the cytosolic compartment. This localization study demonstrates that the C-terminal transmembrane region delivers the protein to mitochondrial outer membranes.

Protein recruitment to mitochondria by Fis1

The structure of Fis1 suggests that it may bind other proteins and recruit them to mitochondria in order to facilitate mitochondria fission. In yeast, Dnm1 and Mdv1 are involved in mitochondria fission, and thought to interact with Fis1.[10–12] The lack of an identifiable Mdv1 homolog in mammals leaves Drp1, a mammalian homolog of Dnm1, as the sole candidate for a binding partner of Fis1. To determine if Fis1 recruits Drp1 to mitochondria, we investigated whether overexpression of Fis1 affects the subcellular distribution of Drp1 in HeLa cells. We compared the localization of Drp1 in cells transfected with pcDNA-hFis1 and untransfected cells (Figure 9A). With an endogenous level of Fis1 as seen in untransfected cells, endogenous Drp1 is partly cytosolic and partly

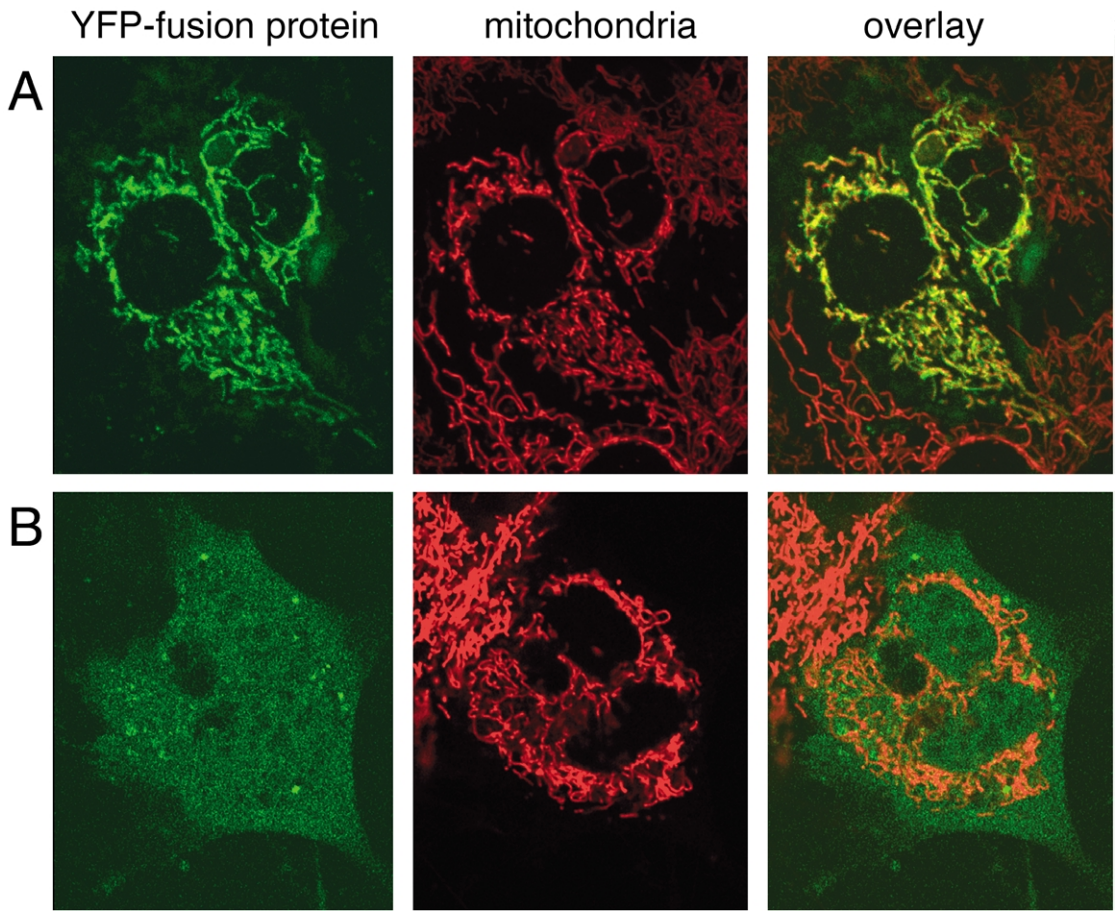

Figure 8. Subcellular localization of Fis1 with or without the C-terminal hydrophobic tail. Cells were transfected with plasmids encoding yellow fluorescence protein (YFP) fused to either (A) wild-type human Fis1 or (B) human Fis1 lacking the C-terminal 30 residues (Leu123-Ser152–COOH), and treated with MitoTracker Red CMXRos. Location of YFP-fusion proteins (green) and mitochondria (red) in cells was visualized by confocal microscopy. Images were overlaid to examine co-localization (yellow) of YFP-fusion protein and mitochondria.

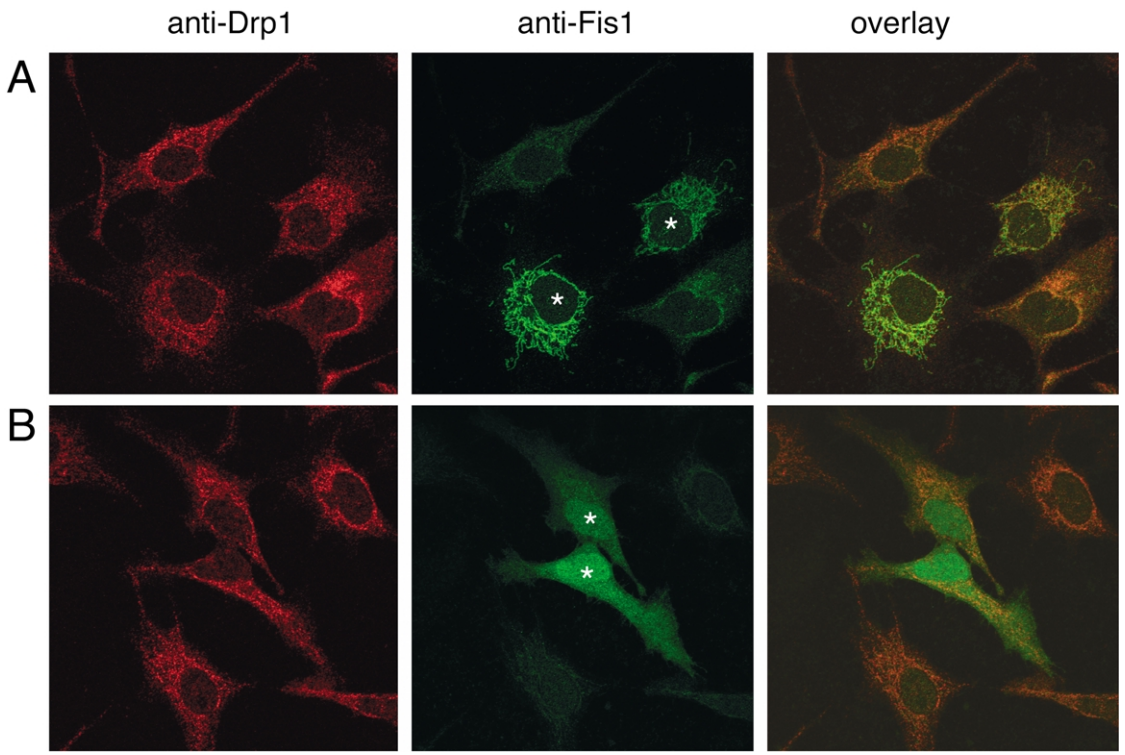

Figure 9. Subcellular distribution of endogenous Drp1 in cells expressing different levels of Fis1. Cells were transfected with plasmids encoding either (A) wild-type human Fis1 or (B) human Fis1 lacking the C-terminal 30 residues (Leu123-Ser152–COOH). Intracellular locations of Drp1 (red) and Fis1 (green) were detected using anti-Drp1 and anti-Fis1 antibodies, respectively. Images were overlaid to examine co-localization (yellow) of Drp1 and Fis1. Cells transfected with pcDNA-hFis1 were marked with asterisks.

localized to mitochondria, which is consistent with a previous report.[8] Cells transfected with pcDNA-hFis1 show increased expression of mitochondria-associated Fis1. However, levels of mitochondria-associated Drp1 did not change. We also tested if overexpression of a C-terminally truncated form of Fis1, that does not dock to mitochondria and would be presumably inactive, would act as a dominant negative inhibitor of fission by binding to Drp1 and preventing its interaction with endogenous Fis1. However, we saw no effect of a C-terminally truncated Fis1 on the subcellular distribution of Drp1 (Figure 9B). Interestingly, elevated levels of Fis1 in the mitochondrial membrane do not cause excessive mitochondrial fission (Figures 8A and 9A), whereas reduction of Fis1 by RNAi results in mitochondria elongation (S.-Y.J. *et al.*, unpublished results). This study suggests that, although Fis1 is required for the mitochondrial fission, the level of mitochondrial Fis1 is not a limiting factor in the mitochondrial fission process and that a possible binding between Drp1 and Fis1 is regulated by other element(s) or a preceding event.

Discussion

Fis1 is required for the proper division of mitochondria. Yeast Fis1 is the only functionally characterized member among the many orthologs. Yeast Fis1, an integral membrane protein localized to the mitochondrial outer membrane, recruits Dnm1 and Mdv1 to fission sites on the mitochondrial outer membrane. However, it has not been characterized how Fis1 recruits other proteins. Although human Fis1 is suggested to have the same function as yeast Fis1, it is currently unknown what human Fis1 recruits to the mitochondria. It is helpful to consider the protein structure of Fis1 in order to investigate the detailed molecular mechanism by which Fis1 functions during mitochondrial fission. The solution structure of Fis1 presents folding similarities to known structural domains that are responsible for protein–protein interaction, including mitochondrial outer membrane import proteins Tom20[23] and Tom70.[25] This folding similarity explains a potential mechanism for Fis1 function in recruiting other proteins involved in mitochondrial fission.

Some structural studies have explored how proteins structurally similar to Fis1 recognize and interact with their target proteins. The C-terminal domain of PEX5 binds the PTS1-containing pentapeptide at the concave side of TPRs 5–7.[17] 14-3-3 forms a cup-shaped structure, and binds phosphoserine peptides at the inner-cup sides.[21] TOM20 binds a presequence peptide within two helix-turn-helix hairpins.[22] In all cases, binding to

peptides occurs at the concave side of the protein, and the peptide–protein binding occurs primarily through hydrophobic interaction. Additional recognitions appear due to electrostatic interactions, hydrogen bonds, as well as sterical fit. Such a mechanism should also apply to the case of Fis1. The concave side of the Fis1 core domain shows a hydrophobic groove (Figure 7). We predict that this groove serves as a binding interface to target proteins. Our NMR data also indirectly suggest this possibility. For the protein in solution, transient interactions between the groove and the C-terminal tail were predicted from NOE data and relaxation data. This possibility could be explained by a hydrophobic interaction. The lack of stable contact may result from lack of additional stabilizing forces such as ionic interaction or from an improper fit of the C-terminal tail into the groove. Despite what was seen for the recombinant protein in solution, the interaction between the groove and the C-terminal tail in living cells is generally excluded because the C-terminal tail intercalates into the mitochondrial outer membrane and therefore is not accessible for the binding. In the native conformation the groove is predicted to be accessible for binding to target proteins.

The C-terminal tail has features found in many tail-anchored mitochondrial proteins, a continuous stretch of hydrophobic amino acid residues sandwiched between positively charged amino acid residues.[24] Well studied C-terminal tail-anchored proteins with this feature include Vamp-1B, monoamine oxidase, and many members in the Bcl-2 family.[26–29] It should be noted that sequence similarity or consensus residues are not found within the hydrophobic stretch of these proteins. However, the length of the hydrophobic stretch does seem important.[29] It is interesting to note that naturally existing splicing variants Vamp-1A and Vamp-1B differ only in a few C-terminal end residues (Ile114-Tyr-Phe-Phe-Thr118–COOH and Arg114-Arg-Asp116–COOH) that differentiate their subcellular localization to membranes of the secretory pathway and mitochondrial membranes.[26] The C-terminal end sequences, Ser148-Lys-Ser-Lys-Ser152–COOH of human Fis1 and Arg151-Asn-Lys-Arg-Arg155–COOH of yeast Fis1, would be predicted as essential for the strict targeting to the mitochondria.

The structural composition of Fis1 that consists of a TPR-like domain and a mitochondrial transmembrane segment suggests that Fis1 probably functions as a molecular adaptor at the mitochondrial outer membrane. On the basis of the sequence similarity, yeast Fis1 is expected to contain a similar TPR-like domain. In such a case, the interaction between Fis1 and Mdv1 or between Fis1 and Dnm1 can be explained by the structure-based functional model of Fis1. It has been reported that a mutation in yeast Fis1 (Leu80 to Pro), corresponding to Val74 within the TPR-like domain of human Fis1, abolishes the interaction between Fis1 and Mdv1 and results in inhibition of mitochondrial fission.[12] This supports the model of protein–protein interaction at the TPR-like domain of Fis1, predicted from the structural similarity to the TPR containing proteins. The authors also indicated that the mutation in yeast Fis1 did not change Dnm1 assembly into punctate structures.[12] Likewise in mammalian cells, Drp1 distribution did not alter by changing the Fis1 protein level, suggesting an involvement of another protein, such as yeast Mdv1, at a distinct stage of mitochondrial fission in mammalian systems.

Common features in the target peptides of TPR domains have not been identified. Binding preference is probably decided by the charge distribution in the perimeter of the hydrophobic groove as well as the shape of the groove that is present at the concave side of a TPR domain. These requirements for Fis1 interaction with its binding partner could provide specificity in its function in mitochondrial fission. Although a Mdv1 homolog has not been found in mammals by overall sequence similarity, it is possible that a yet-unknown protein functionally similar to Mdv1 contains a short sequence that fits in the binding groove of mammalian Fis1, and that the Mdv1-like protein is required to facilitate mitochondrial fission in the mammalian system. Future studies should include the discovery of Fis1-binding partners in mammalian cells, followed by understanding the mechanism of partner recognition along the mitochondrial fission process.

Materials and Methods

Cloning and recombinant protein

The cDNA of human Fis1 was obtained from cDNA libraries of human hepatocellular carcinoma Hep G2 cells, and of fetal human brain mRNA (Straragene). For the recombinant protein, a nonsense mutation (cytidine 174 to guanosine) was made to eliminate the *Xho*I site within the cDNA, followed by mutations (G^{-3}CCATG^{3} to CATATG and C^{433}TTGCT^{439} to CTCGAG) in order to introduce *Nde*I and *Xho*I sites. The fragment and pET21b vector (Novagen Inc.) were treated with *Nde*I and *Xho*I, then ligated. The resulting plasmid pET21-hFis1-His_6 encodes human Fis1 protein, the length of which is exactly the same as the wild-type protein and the C terminus of which was substituted from Ala146-Val-Ser-Lys-Ser-Lys-Ser152–COOH to Glu-His-His-His-His-His-His–COOH.

NMR sample

Escherichia coli BL21(DE3) harboring the plasmid pET21-hFis1-His_6 was cultured in Martek-9N medium (Spectra Stable Isotopes) to produce uniformly ^{15}N-labeled protein. Martek-9CN medium was used for uniformly ^{15}N-, ^{13}C-labeled protein, and a minimal medium containing 10% [U-^{13}C]glucose–90% [U-^{12}C]-glucose was used for 10% ^{13}C-labeled protein.[30]

The recombinant proteins were isolated from the cytosol by a metal chelate affinity chromatography on a Ni^{2+}-resin column (Novagen Inc.), then further purified

by an ion-exchange chromatography on a mono-Q column (Amersham Pharmacia Biotech). The proteins were bound to a Ni^{2+}-resin column using 20 mM Tris–HCl (pH 7.9), 500 mM NaCl, and eluted with the buffer containing 100 mM EDTA. Then, the proteins were bound to a mono-Q column using 20 mM Tris–HCl, pH 8.0, and eluted with a linear gradient of NaCl. No detergents were used in any step of the protein purification. The purified proteins were confirmed using SDS-PAGE, gel filtration chromatography, and mass spectrometry. The recombinant proteins were concentrated to 0.5–1.0 mM in 10 mM Tris–acetate pH 5.5 in 90% H_2O/10% ^2H_2O or 100% ^2H_2O.

NMR spectroscopy

All NMR spectra were acquired at 32 °C on Bruker 600 MHz or 800 MHz NMR spectrometers. The spectra were processed using the NMRPipe[31] and analyzed with PIPP.[32] The following experiments were used for assignments of ^1H, ^{13}C and ^{15}N resonances; CBCA(CO)NH,[33] HNCACB,[34] HBHA(CO)NH,[35] HNCO,[36] and 3D HCCH-TOCSY.[37] For stereospecific assignment for methyl groups of leucine residues and valine residues, a ^1H–^{13}C CT-HSQC experiment[38] was carried out using the 10% ^{13}C-labeled protein.[30] Proton homonuclear NOEs were obtained using 3D ^{15}N-edited NOESY,[35] 4D ^{15}N/^{13}C-edited NOESY,[39] and 4D ^{13}C/^{13}C-edited NOESY[40] experiments.

Residual dipolar couplings for N–H vectors ($^1D_{N-H}$) were calculated from the difference in corresponding scalar couplings ($^1J_{N-H}$) measured in the presence and absence of 5% bicelle. The bicelles were generated by a mixture of dimyristoyl phosphatidylcholine and dihexanoyl phosphatidylcholine (Avanti Polar Lipids, Inc.) at 3:1 molar ratio. A 2D IPAP ^{15}N–^1H HSQC experiment[41] was used to obtain the one-bond N–H scalar coupling ($^1J_{N-H}$) values.

Amide ^{15}N T_2 values were derived from amide ^{15}N $T_{1\rho}$ spectra measured using conventional pulse sequence.[42] The measurements were repeated twice at 32 °C in the field strength of 800 MHz.

Structure calculation and presentation

Regions of regular secondary structure were determined based on secondary $^{13}C^{\alpha}$ chemical shifts and medium range NOE patterns. The TALOS program[15] was used to predict dihedral angles ϕ and ψ. The statistically significant angles in regular secondary structure were used as structural restraints. Generic hydrogen bond distance restraints were employed for α-helical regions. Peak intensities from NOESY experiments were translated into a continuous distribution of proton–proton distances. Structures of human Fis1 were calculated by a distance geometry and simulated annealing protocol[43] with the incorporation of dipolar coupling restraints[44] using the program XPLOR-NIH.[45] Structure calculations employed 2000 inter-residue and 742 intra-residue proton–proton distance restraints, 138 hydrogen bond distance restraints, 87 ϕ and 87 ψ angle restraints, 67 N–H dipolar couplings.

Figures for protein structure presentation were prepared using MOLMOL[46] for Figures 4 and 7, or MOLSCRIPT[47] for Figure 5.

Detection of Fis1 and Drp1 in cells

The cDNA for full-length or residues Met1-Gly122 of human Fis1 was subcloned into *Eco* RI and *Kpn* I sites of pEYFP-C3 plasmid vector (Clontech Laboratories, Inc.) or pcDNA3.1 plasmid vector (Invitrogen). HeLa cells (American Type Culture Collection) were transfected with the pEYFP-hFis1 or pcDNA-hFis1 constructs using FuGENE transfection reagent (Roche Diagnostics GmbH) as described. After 18 hours, live cells transfected with pEYFP constructs were treated with a mitochondrion-specific dye (MitoTracker Red CMXRos; Molecular Probes Inc.). Cells transfected with pcDNA constructs were fixed using 4% (v/v) paraformaldehyde, permealized using 0.15% (v/v) Triton X-100, then probed with anti-Drp1 monoclonal antibody (anti-DLP1 clone 8, BD Transduction Laboratory) followed by anti-mouse Alexa Fluor 594 (Molecular Probes, Inc.), and anti-Fis1 polyclonal antibody raised against the peptide corresponding to residues Leu62-Tyr76 of human Fis1 (Covance) followed by anti-rabbit Alexa Fluor 488. All images were collected using a confocal microscope (LSM 510, Carl Zeiss).

Structure coordinates

The coordinates for the 20 lowest energy structures of human Fis1 have been deposited to the PDB with the accession number 1PC2.

Acknowledgements

We thank Drs Amotz Nechushtan (Biochemistry Section, NINDS), Eva de Alba, Shou-Lin Chang (Laboratory of Biophysical Chemistry, NHLBI), Dan Garret (Laboratory of Chemical Physics, NIDDK) for technical assistance, Drs James W. Nagle & Deborah Kauffman (NINDS DNA sequencing facility) for DNA sequencing, and Drs Henry M. Fales & Fuquan Yang (Laboratory of Biophysical Chemistry, NHLBI) for mass spectrometry analysis.

References

1. Santel, A. & Fuller, M. T. (2001). Control of mitochondrial morphology by a human mitofusin. *J. Cell Sci.* **114**, 867–874.
2. Hales, K. G. & Fuller, M. T. (1997). Developmentally regulated mitochondrial fusion mediated by a conserved, novel, predicted GTPase. *Cell*, **90**, 121–129.
3. Hermann, G. J., Thatcher, J. W., Mills, J. P., Hales, K. G., Fuller, M. T., Nunnari, J. & Shaw, J. M. (1998). Mitochondrial fusion in yeast requires the transmembrane GTPase Fzo1p. *J. Cell Biol.* **143**, 359–373.
4. Rapaport, D., Brunner, M., Neupert, W. & Westermann, B. (1998). Fzo1p is a mitochondrial outer membrane protein essential for the biogenesis of functional mitochondria in *Saccharomyces cerevisiae*. *J. Biol. Chem.* **273**, 20150–20155.
5. Otsuga, D., Keegan, B. R., Brisch, E., Thatcher, J. W., Hermann, G. J., Bleazard, W. & Shaw, J. M. (1998). The dynamin-related GTPase, Dnm1p, controls

mitochondrial morphology in yeast. *J. Cell Biol.* **143**, 333–349.
6. Bleazard, W., McCaffery, J. M., King, E. J., Bale, S., Mozdy, A., Tieu, Q. *et al.* (1999). The dynamin-related GTPase Dnm1 regulates mitochondrial fission in yeast. *Nature Cell Biol.* **1**, 298–304.
7. Sesaki, H. & Jensen, R. E. (1999). Division *versus* fusion: Dnm1p and Fzo1p antagonistically regulate mitochondrial shape. *J. Cell Biol.* **147**, 699–706.
8. Smirnova, E., Griparic, L., Shurland, D. L. & van der Bliek, A. M. (2001). Dynamin-related protein Drp1 is required for mitochondrial division in mammalian cells. *Mol. Biol. Cell*, **12**, 2245–2256.
9. Frank, S., Gaume, B., Bergmann-Leitner, E. S., Leitner, W. W., Robert, E. G., Catez, F. *et al.* (2001). The role of dynamin-related protein 1, a mediator of mitochondrial fission, in apoptosis. *Dev. Cell*, **1**, 515–525.
10. Mozdy, A. D., McCaffery, J. M. & Shaw, J. M. (2000). Dnm1p GTPase-mediated mitochondrial fission is a multi-step process requiring the novel integral membrane component Fis1p. *J. Cell Biol.* **151**, 367–379.
11. Tieu, Q. & Nunnari, J. (2000). Mdv1p is a WD repeat protein that interacts with the dynamin-related GTPase, Dnm1p, to trigger mitochondrial division. *J. Cell Biol.* **151**, 353–365.
12. Tieu, Q., Okreglak, V., Naylor, K. & Nunnari, J. (2002). The WD repeat protein, Mdv1p, functions as a molecular adaptor by interacting with Dnm1p and Fis1p during mitochondrial fission. *J. Cell Biol.* **158**, 445–452.
13. Blatch, G. L. & Lassle, M. (1999). The tetratricopeptide repeat: a structural motif mediating protein–protein interactions. *BioEssays*, **21**, 932–939.
14. Lamb, J. R., Tugendreich, S. & Hieter, P. (1995). Tetratrico peptide repeat interactions-to TPR or Not to TPR. *Trends Biochem. Sci.* **20**, 257–259.
15. Cornilescu, G., Delaglio, F. & Bax, A. (1999). Protein backbone angle restraints from searching a database for chemical shift and sequence homology. *J. Biomol. NMR*, **13**, 289–302.
16. Holm, L. & Sander, C. (1993). Protein–structure comparison by alignment of distance matrices. *J. Mol. Biol.* **233**, 123–138.
17. Gatto, G. J., Geisbrecht, B. V., Gould, S. J. & Berg, J. M. (2000). Peroxisomal targeting signal-1 recognition by the TPR domains of human PEX5. *Nature Struct. Biol.* **7**, 1091–1095.
18. Das, A. K., Cohen, P. T. W. & Barford, D. (1998). The structure of the tetratricopeptide repeats of protein phosphatase 5: implications for TPR-mediated protein–protein interactions. *EMBO J.* **17**, 1192–1199.
19. Rice, L. M. & Brunger, A. T. (1999). Crystal structure of the vesicular transport protein Sec17: implications for SNAP function in SNARE complex disassembly. *Mol. Cell*, **4**, 85–95.
20. Steegborn, C., Danot, O., Huber, R. & Clausen, T. (2001). Crystal structure of transcription factor MaIT domain III: a novel helix repeat fold implicated in regulated oligomerization. *Structure*, **9**, 1051–1060.
21. Rittinger, K., Budman, J., Xu, J. A., Volinia, S., Cantley, L. C., Smerdon, S. J. *et al.* (1999). Structural analysis of 14-3-3 phosphopeptide complexes identifies a dual role for the nuclear export signal of 14-3-3 in ligand binding. *Mol. Cell*, **4**, 153–166.
22. Abe, Y., Shodai, T., Muto, T., Mihara, K., Torii, H., Nishikawa, S. *et al.* (2000). Structural basis of presequence recognition by the mitochondrial protein import receptor Tom20. *Cell*, **100**, 551–560.
23. Iwahashi, J., Yamazaki, S., Komiya, T., Nomura, N., Nishikawa, S., Endo, T. & Mihara, K. (1997). Analysis of the functional domain of the rat liver mitochondrial import receptor Tom20. *J. Biol. Chem.* **272**, 18467–18472.
24. Wattenberg, B. & Lithgow, T. (2001). Targeting of C-terminal (tail)-anchored proteins: understanding how cytoplasmic activities are anchored to intracellular membranes. *Traffic*, **2**, 66–71.
25. Young, J. C., Hoogenraad, N. J. & Hartl, F. U. (2003). Molecular chaperones Hsp90 and Hsp70 deliver preproteins to the mitochondrial import receptor Tom70. *Cell*, **112**, 41–50.
26. Isenmann, S., Khew-Goodall, Y., Gamble, J., Vadas, M. & Wattenberg, B. W. (1998). A splice-isoform of vesicle-associated membrane protein-1 (VAMP-1) contains a mitochondrial targeting signal. *Mol. Biol. Cell*, **9**, 1649–1660.
27. Mitoma, J. & Ito, A. (1992). Mitochondrial targeting signal of rat-liver monoamine oxidase-B is located at its carboxy terminus. *J. Biochem. (Tokyo)*, **111**, 20–24.
28. Nguyen, M., Millar, D. G., Yong, V. W., Korsmeyer, S. J. & Shore, G. C. (1993). Targeting of Bcl-2 to the mitochondrial outer-membrane by a COOH-terminal signal anchor sequence. *J. Biol. Chem.* **268**, 25265–25268.
29. Kaufmann, T., Schlipf, S., Sanz, J., Neubert, K., Stein, R. & Borner, C. (2003). Characterization of the signal that directs Bcl-X_L, but not Bcl-2, to the mitochondrial outer membrane. *J. Cell Biol.* **160**, 53–64.
30. Neri, D., Szyperski, T., Otting, G., Senn, H. & Wuthrich, K. (1989). Stereospecific nuclear magnetic-resonance assignments of the methyl-groups of valine and leucine in the DNA-binding domain of the 434-repressor by biosynthetically directed fractional ^{13}C labeling. *Biochemistry*, **28**, 7510–7516.
31. Delaglio, F., Grzesiek, S., Vuister, G. W., Zhu, G., Pfeifer, J. & Bax, A. (1995). NMRPipe—a multidimensional spectral processing system based on Unix pipes. *J. Biomol. NMR*, **6**, 277–293.
32. Garrett, D. S., Powers, R., Gronenborn, A. M. & Clore, G. M. (1991). A common-sense approach to peak picking in 2-dimensional, 3-dimensional, and 4-dimensional spectra using automatic computer-analysis of contour diagrams. *J. Magn. Reson.* **95**, 214–220.
33. Grzesiek, S. & Bax, A. (1992). Correlating backbone amide and side-chain resonances in larger proteins by multiple relayed triple resonance NMR. *J. Am. Chem. Soc.* **114**, 6291–6293.
34. Wittekind, M. & Mueller, L. (1993). HNCACB, a high-sensitivity 3D NMR experiment to correlate amide-proton and nitrogen resonances with the alpha-carbon and beta-carbon resonances in proteins. *J. Magn. Reson. ser. B*, **101**, 201–205.
35. Bax, A. & Grzesiek, S. (1993). Methodological advances in protein NMR. *Acc. Chem. Res.* **26**, 131–138.
36. Kay, L. E., Xu, G. Y. & Yamazaki, T. (1994). Enhanced-sensitivity triple-resonance spectroscopy with minimal H_2O saturation. *J. Magn. Reson. ser. A*, **109**, 129–133.
37. Bax, A., Clore, G. M. & Gronenborn, A. M. (1990). ^1H–^1H correlation *via* isotropic mixing of ^{13}C magnetization, a new 3-dimensional approach for assigning

^{1}H and ^{13}C spectra of ^{13}C-enriched proteins. *J. Magn. Reson.* **88**, 425–431.
38. Vuister, G. W. & Bax, A. (1992). Resolution enhancement and spectral editing of uniformly ^{13}C-enriched proteins by homonuclear broad-band ^{13}C decoupling. *J. Magn. Reson.* **98**, 428–435.
39. Kay, L. E., Clore, G. M., Bax, A. & Gronenborn, A. M. (1990). 4-Dimensional heteronuclear triple-resonance NMR-spectroscopy of Interleukin-1β in solution. *Science*, **249**, 411–414.
40. Clore, G. M., Kay, L. E., Bax, A. & Gronenborn, A. M. (1991). 4-Dimensional ^{13}C/^{13}C-edited Nuclear Overhauser Enhancement spectroscopy of a protein in solution—application to Interleukin 1β. *Biochemistry*, **30**, 12–18.
41. Ottiger, M., Delaglio, F. & Bax, A. (1998). Measurement of *J* and dipolar couplings from simplified two-dimensional NMR spectra. *J. Magn. Reson.* **131**, 373–378.
42. Barbato, G., Ikura, M., Kay, L. E., Pastor, R. W. & Bax, A. (1992). Backbone dynamics of Calmodulin studied by ^{15}N-relaxation using inverse detected 2-dimensional NMR-spectroscopy—the central helix is flexible. *Biochemistry*, **31**, 5269–5278.
43. Kuszewski, J., Nilges, M. & Brunger, A. T. (1992). Sampling and efficiency of metric matrix distance geometry—a novel partial metrization algorithm. *J. Biomol. NMR*, **2**, 33–56.
44. Tjandra, N., Omichinski, J. G., Gronenborn, A. M., Clore, G. M. & Bax, A. (1997). Use of dipolar ^{1}H–^{15}N and ^{1}H–^{13}C couplings in the structure determination of magnetically oriented macromolecules in solution. *Nature Struct. Biol.* **4**, 732–738.
45. Schwieters, C. D., Kuszewski, J. J., Tjandra, N. & Clore, G. M. (2003). The Xplor-NIH NMR molecular structure determination package. *J. Magn. Reson.* **160**, 65–73.
46. Koradi, R., Billeter, M. & Wuthrich, K. (1996). MOLMOL: a program for display and analysis of macromolecular structures. *J. Mol. Graph.* **14**, 51–55.
47. Kraulis, P. J. (1991). Molscript—a program to produce both detailed and schematic plots of protein structures. *J. Appl. Crystallog.* **24**, 946–950.
48. Yoon, Y., Krueger, E. W., Oswald, B. J. & McNiven, M. A. (2003). The mitochondrial protein hFis1 regulates mitochondrial fission in mammalian cells through an interaction with the dynamin-like protein DLP1. *Mol. Cell. Biol.* **23**, 5409–5420.
49. Thompson, J. D., Higgins, D. G. & Gibson, T. J. (1994). Clustal-W—improving the sensitivity of progressive multiple sequence alignment through sequence weighting, position-specific gap penalties and weight matrix choice. *Nucl. Acids Res.* **22**, 4673–4680.

Edited by M. F. Summers

(Received 3 June 2003; received in revised form 13 September 2003; accepted 24 September 2003)

Note added in proof: Since submission of this manuscript, related work was published. Yoon *et al*.[48] reported that microinjection of an antibody to the residues 12–38 disrupts human Fis1 function, suggesting a steric hindrance of a possible protein–protein interaction at the core domain containing the TPR-motifs. The paper also describes that a direct interaction between Fis1 and Drp1 can be detected only in the presence of a cross-linker, suggesting that the interaction is weak, unstable and/or transient.